

HYGROTHERMAL BEHAVIOUR OF HOLLOW AND FILLED CERAMIC MASONRY BLOCKS

Balázs Nagy⁽¹⁾, Elek Tóth⁽¹⁾

(1) Budapest University of Technology and Economics, Budapest, Hungary

Abstract

Nowadays energy- and comfort-conscious design approach of buildings necessitates the development of the masonry blocks as well. The building blocks with different internal structures and various fillers are rapidly spread the market. The study deals with heat and moisture migration problems within these blocks. The aim of the research is to analyse selected 30 cm, 38 cm and 44 cm thick hollow and filled ceramic masonry blocks, using different filler materials, such as stone wool, expanded perlite and polyurethane foam. The comparison based on multi-dimensional HAM simulations of the building blocks, in which case the material properties are specified by laboratory tests. The steady-state models are compared to measurements and simulations performed on masonry blocks' sections also. For the transient conjugated heat, air and moisture transfer simulations, different climate conditions (Budapest, Espoo, Lisbon) across Europe are used. During the research, 4 different masonry block types and 5 different fillers were analysed and compared.

1. Introduction

Ceramic brick as building material has been used for thousands of years. By the 19th century, because of the mechanized form of mass production, bricks became the most popular building material of industrial and commercial buildings. In the 20th century, new manufacture procedures and new brick products have been developed, such as lightweight bricks. Lightweight bricks are made of expanded clay aggregate. During the manufacture process the clay that is mixed with water is forced through an opening, which called a "die" and results continuous formed brick ribbon called "column" [1]. Then it is cut into pieces with necessary sizes. The cut bricks are hardened by drying at 50 to 150°C and then fired. The die is also suitable to create perforations into the clay bricks. These hollows reduce the volume of clay needed, and also increase the thermal performance. Hollow bricks are lighter, therefore easier to handle, and usually used in single-wall constructions with finishes applied on the

inside and outside. From the point of our research, the development of hollow or filled masonry blocks is significant only after the 1960-s in Europe. Consequently the development of bricks occurred in two directions, after and regarding to the oil crisis in the 1970-s. The manufacturers started increasing the size of the holes, therefore decreasing the mass, as well as increasing the size of blocks to make the construction process more efficient and applying more porous material with smaller thickness. In case of perforated bricks, the location of holes has an effect on the thermal performance. For example a zigzag design results in a longer route for the heat transfer, therefore increases the thermal resistance. Beside the location, the different shapes of the holes also influence the heat transfer; therefore it has to be investigated. Nowadays, the energy performance requirements are more and more rigorous, so manufacturers increase the thermal resistance of blocks with different fillings in the holes: such as mineral wool, perlite or graphite expanded polystyrene (EPS) foam (Fig. 1). Since the air can move in the holes, most of the solid insulating materials have lower thermal conductivities than the moving air's equivalent value in the gaps of the building blocks. Using fillings in the holes can lead to better thermal insulating capability [2].



Figure 1. Filled ceramic building blocks, left to right: Mineral wool (Porotherm Thermo), Graphite EPS foam (Leier ISO+), Perlite (Poroton T8)

In this article four different building blocks with four different hollow shapes: rhombus, small rectangular, triangular and small rectangular, and big rectangular are investigated, and we also analyse the effect of fillers: air, expanded perlite, mineral wool, PUR foam and aerogel.

2. LABORATORY MEASUREMENTS OF MATERIALS

2.1 Materials

In the research, we used fired clay masonry blocks. The fired clay is mineral aggregate composed of hydrous silicates of aluminium ($\text{Al}_2\text{O}_3 \cdot 2\text{SiO}_2 \cdot 2\text{H}_2\text{O}$) with or without free silica. In the masonry block industry, manufacturers trying to reduce the density of their clay units, of course taking into consideration of the attendant degradation of the mechanical properties. For the fillers, we used air, which is obviously the cheapest filler, expanded perlite, mineral wool, PUR foam and aerogel particles as well.

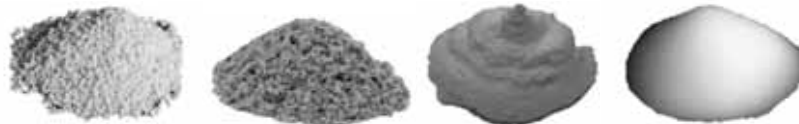


Figure 2. Fillers, left to right: Expanded perlite, Mineral wool, PUR foam, Aerogel particles

2.2 Measured hygrothermal properties

The measurements performed at the Department of Construction Materials and Technologies, Laboratory of Building Physics. We measured each material's ρ density, λ thermal conductivity (for the temperature and moisture dependency, we used EN ISO 10456:2007 model), moisture storage curve and μ vapour diffusion resistance factor.



Figure 3. Left to right: Taurus guarded hot plate apparatus; Sorption curve measurement in insulated chambers; Labmaster-aw instrument; Vapour diffusion measurements.

We get c_p specific heat capacity from EN ISO 10456:2007 except for aerogel [3]. The “K” permeability of the materials are set to 5 kg/msPa for fired clay and 0.001 kg/msPa for loose-filled insulation materials. The hygrothermal properties of air in the hollows are related to the temperature and to the width of the layer according to EN ISO 6946:2007 and [4]. The specimens' thermal conductivity was tested using a Taurus TLP 300 DTX single-specimen apparatus (Fig.3) according to EN 12664:2001 and EN 12667:2001. The loose-filled 20 cm x 20 cm x 5 cm specimens were framed by 10 cm thick EPS 200 foam stocks, ensuring that the temperature or humidity in the lab do not affect the results of the measurements and in the specimens measured intermediate 10 cm x 10 cm area, one-dimensional steady state heat flow can develop during all three measured temperature stages. Between the samples and the EPS frame, we taped aluminium foil moisture and vapour barrier layer. For the measurement, 1 – 1 cm thick EPS200 layer were added to the top and bottom of the sample to reduce the measurement errors which occurs using guarded hot plate measurement. The process is shown in Fig. 4. Later, the effect of the EPS 200 layers were calculated and compensated back.



Figure 4. Left to right: Hot wire EPS cutter; EPS stock with Al foil; Perlite filled stock in apparatus; pressed specimen in apparatus with both (hot & cold side) thermocouples on place.

We measured μ of the materials according to EN ISO 12572:2001 in dry-cup conditions using salt solutions which forms a pressure difference between the two sides of the specimen; therefore we can measure the water vapor diffusion through the material. The instruments and the measurement setup used is shown in Fig. 3.

Table 1: Material properties

	Fired clay	Expanded perlite	Mineral Wool	PUR foam	Aerogel
ρ (kg/m ³)	1500	90	75	35	120
λ (W/mK)	0.35	0.05	0.031	0.024	0.012
c_p (J/kgK)	800	900	1000	1400	1000
f_T (1/K)	0.0010	0.0035	0.0045	0.0055	0.0015
f_ψ (m ³ /m ³)	10	3	4	6	3
μ (-)	15	2	1.3	60	4.5

The moisture storage curves measured between the range of 0-97 % RH according to EN ISO 12571:2013 and after we can obtain the free water saturation point by immersing the samples in water for 28 days. It is observable (Fig. 5.) that our PUR foam is not a hydrophobic filler.

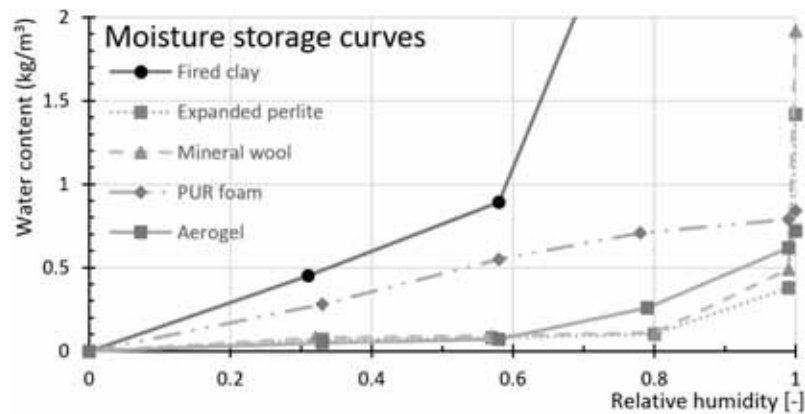


Figure 5. Moisture storage curves of fired clay and filler materials.

For the HAM simulations, D diffusion coefficient (m²/s) calculated according to [5, 6]:

$$D = \frac{p_{v,sat}(T) \cdot \delta_{air}(T)}{\mu \cdot \xi(RH)} \quad (1)$$

Where $p_{v,sat}$ is the saturation vapor pressure related to temperature (Pa), δ_{air} is the water vapor diffusion coefficient in air related to temperature (kg/smPa) and ξ is the specific moisture capacity related to RH (kg/m³).

3. CONJUGATED HEAT, AIR & MOISTURE TRANSPORT

3.1 Partial differential equations

The PDE's based on [7, 8] for heat- (eq.2), air- (eq.3) and moisture transfer (eq.4) are:

$$\rho C_p \frac{\partial T}{\partial t} + \nabla \cdot (-\lambda \nabla T) + \rho C_p \mathbf{u} \cdot \nabla T = 0 \quad (2)$$

$$\frac{\partial P}{\partial t} + \nabla \cdot (-K \nabla P) = 0; \mathbf{u} = K \nabla P \quad (3)$$

$$\frac{\partial p_v}{\partial t} + \nabla \cdot (-D \nabla p_v) + \mathbf{u} \cdot \nabla p_v = 0 \quad (4)$$

Where \mathbf{u} is the air velocity (m/s), P is the (scaled) atmospheric pressure (Pa), p_v is the partial vapor pressure (Pa).

3.2 Boundary conditions

The boundary conditions for heat flux (eq. 5) and adiabatic (eq. 6) conditions are:

$$\mathbf{n} \cdot (\lambda \nabla T) = (h_c + h_r) \left(T_{inf} + \frac{a \cdot I}{h_r} - T \right) \quad (5)$$

$$\mathbf{n} \cdot (\lambda \nabla T) = 0 \quad (6)$$

Where h_c is the convective and h_r is the radiative heat transfer coefficient ($\text{W}/\text{m}^2\text{K}$) according to EN ISO 6946:2007, a is the solar absorption coefficient. T_{inf} temperature in steady-state conditions set to 20°C internal and -2°C external according to MSZ 24140:2015 and I solar irradiance on surface (W/m^2) neglected. In transient state, both heat transfer coefficients and sol-air temperature varies over the hourly climate data (temperature, wind speed, radiation).

The pressure (eq. 7) and insulation (eq. 8) boundaries for air transport is set to:

$$P = P_{inf} \quad (7)$$

$$\mathbf{n} \cdot (K \nabla P) = 0 \quad (8)$$

Where P_{inf} set to 0 Pa internal and 2.5 Pa external values based on [7] in steady-state conditions and depending on wind speed in transient state. According to [8, 9 and 10], the moisture transfer conditions are the following:

$$\mathbf{n} \cdot (D \nabla p_v) = \beta_p h_c (p_{v,inf} - p_v) \quad (9)$$

$$\mathbf{n} \cdot (D \nabla p_v) = 0 \quad (10)$$

Where β_p is the relationship between the water vapour transfer coefficient and the convective heat transfer coefficient ($7.7 \cdot 10^{-9} \text{ kgK}/\text{WsPa}$) and $p_{v,inf}$ is the vapor pressure which in steady-state conditions set to internal: $0.65 \cdot p_{v,sat}(20^\circ\text{C})$, and external: $0.9 \cdot p_{v,sat}(-2^\circ\text{C})$ respecting MSZ 24140:2015 Hungarian standard and in transient state, parameters depending on the actual hourly data of relative humidity and temperature.

3.3 Geometry models

Four different types of masonry blocks were modelled in AutoCAD 2015 [11] as shown in Fig. 6. The 30HS is 30 cm x 25 cm x 25 cm and have mostly rhombus based internal structure. The 38A+ is 38 cm x 25 cm x 25 cm and have only small, rectangular based internal hollows. 44T marked block is 44 cm x 25 cm x 25 cm and have triangle and rectangle shaped internal structure. The 44T is the same size as 44K, but with big rectangular hollows.

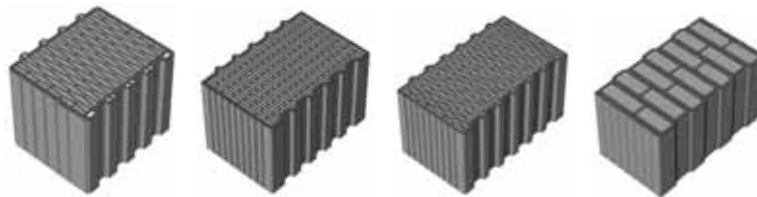


Figure 6. Left to right: 30HS, 38A+, 44K and 44T masonry blocks

4. SIMULATION AND RESULTS

The simulations carried out using Comsol Multiphysics 5.0 [12] using the presented equations in heat transfer, Darcy's law and transport in diluted species coupled physics modules.

4.1 Equivalent thermal conductivity in steady-state conditions

We calculated the equivalent thermal conductivities of the tested masonry blocks. The method is presented in [2] and the steps for the conjugated method shown in Fig. 7.

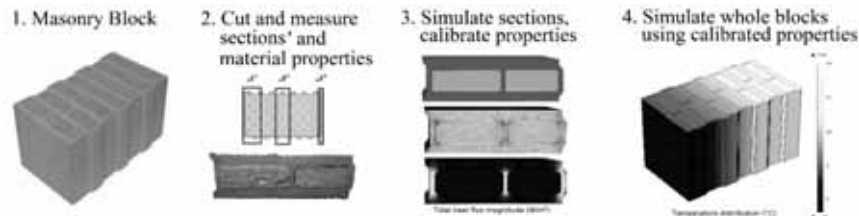


Figure 7. Thermal conductivity evaluation method using measurements and simulations

We are measuring hygrothermal parameters on each material (fired clay and fillers) and block sections to calibrate the material properties and behaviour in simulated sections, and then set the parameters on whole block simulations. Material properties measured both dry and laboratory conditioned (23 °C and 50 % RH). The results are summed in Table 4.

Table 4: Equivalent thermal conductivities (W/mK)

	Air	Exp. Perlite	Mineral Wool	PUR foam	Aerogel
30 HS	0.124	0.108	0.092	0.078	0.058
38 A+	0.115	0.109	0.091	0.074	0.056
44 K	0.111	0.109	0.090	0.073	0.055
44 T	0.263	0.102	0.082	0.070	0.054

4.1 Temperature & RH distribution in steady-state conditions

Due to limited space of the paper, only the results of “44K” masonry blocks presented.

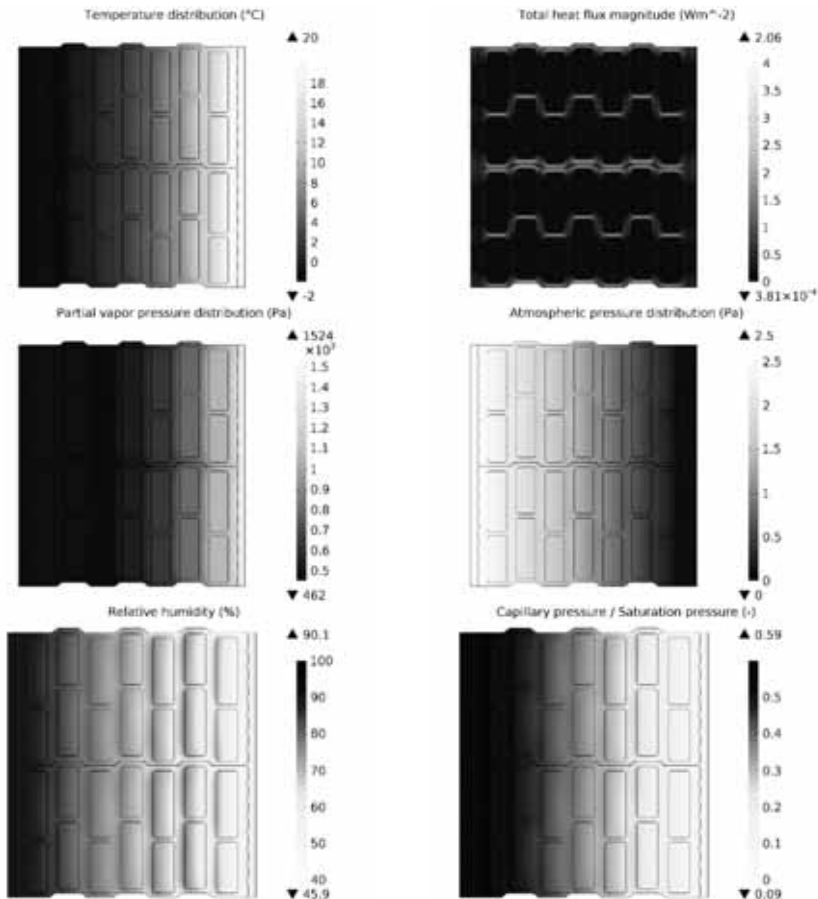


Figure 8. Result of two mineral wool filled 44T blocks with tongue and groove connection

We used 1.5 cm plaster on both sides of the masonry blocks for the temperature and relative humidity distribution analysis, and simulated two blocks connected. It can be observed in Fig. 8. that the heat flux magnitude is showing a dominant path of heat flow in the internal ceramic spacers, and tongue and groove connections. Optimizing the geometry of the internal structure may can lower the thermal conductivity of this block type. The relative humidity in the block is below the saturation level inside the component, but noticeably higher at the outer sides of the insulating layers (see also in Fig. 10). The results also shows, that only hydrophobic fillers (e.g. mineral wool) can be used in these masonry blocks to avoid moisture induced degradation of thermal conductivity. Hydrophobic fillers have significantly lower water content values till 80-90 % RH (see Fig. 5), therefore their thermal conductivities did not raise much in normal operating conditions along the masonry blocks from inside to outside.

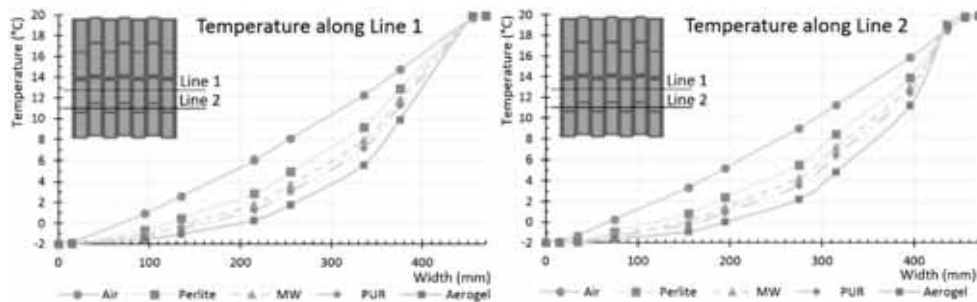


Figure 9. Temperature along line 1 and line 2 through 44T blocks with different fillers

Comparing the different filling materials, the large air hollows are the worst case for temperature distribution (and for thermal conductivity as well, see Table 4.), but gives the best, lowest relative humidity distribution along the blocks as noticeable in Fig. 10. The temperature distribution along line is correlating to the filler materials thermal conductivities, as observable in Fig. 9. Better thermal insulation results lower temperature distribution but higher relative humidity. It is also noticeable that better thermal insulating fillers results greater frost zone (where temperature is below 0 °C) from the outer side of the masonry blocks. When the hollows contain Perlite, the frost zone is 12 cm, but using aerogel gives 20 cm. It can be seen, that relative humidity along line increases more from inside (right side) to outside (left side) when the filler is non-hydrophobic (PUR foam).

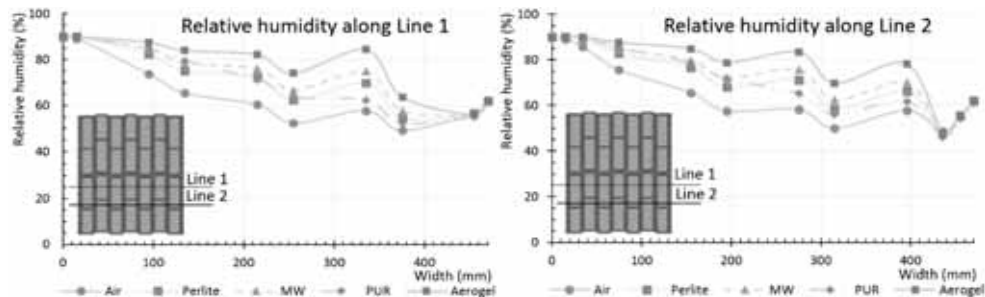


Figure 10. Relative humidity along line 1 and line 2 through 44T blocks with different fillers

4.2 Temperature & RH distribution in transient conditions

In the paper, two transient simulation results are presented from 44T masonry block simulations. The first one shown in Fig. 10. represents a comparison between mineral wool filled 44T model on three different climates, Budapest (Hungary), Espoo (Finland) and Lisbon (Portugal). The climate of Budapest constructed from 2012-2014 data [13, 14], Espoo and Lisbon are from [15]. The simulations were run three years with hourly time-steps, but only the third year appears on Fig. 11 and Fig. 12. Preceding graph shows the mineral wool filled 44T's relative humidity along time in the outermost insulation layer in the block. The average relative humidity in the outermost mineral wool layer is showing correlation with external temperature. Espoo weather are the coldest both in summer and in winter. Budapest have colder winters but hotter summers, than Lisbon.

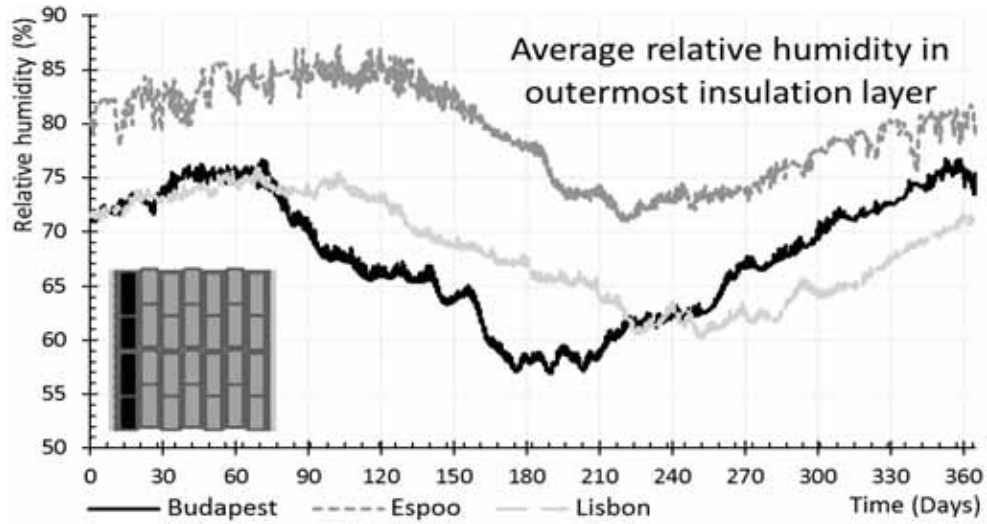


Figure 11. Mineral wool filled 44T masonry block in Budapest, Espoo, Lisbon climate

Fig. 12 shows that different fillers of 44T block behave similarly on the same climate, PUR foam had the lowest average relative humidity values and air had the highest values. It is readable, that in case of climate data in Budapest, none of the fillers have relative humidity values over 80 % which is good, because the filling materials water content (see Fig. 5) doesn't increasing so much causing significant deterioration in thermal properties.

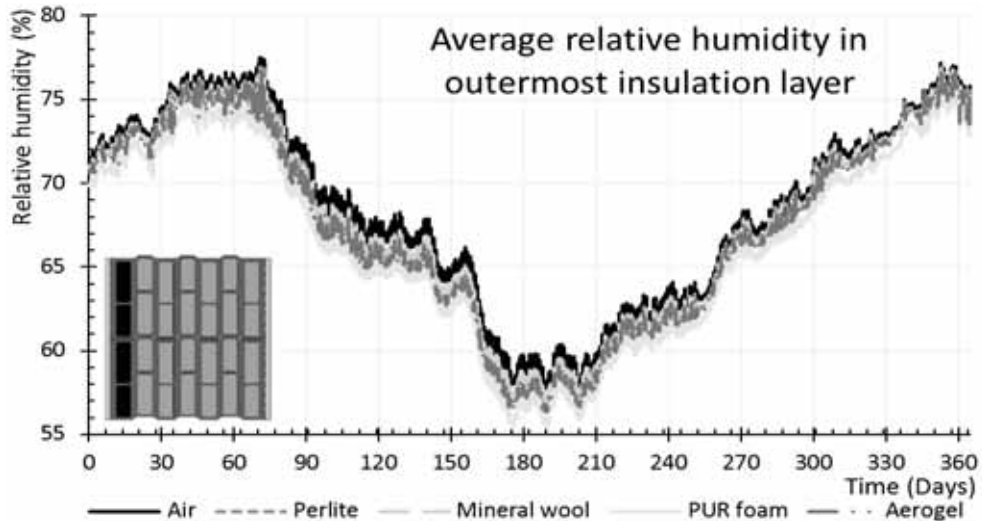


Figure 12. Different (Air, Perlite, MW, PUR, Aerogel) fillers in 44T block, Budapest climate

5. CONCLUSIONS

In this paper, four types of masonry blocks with five different filling materials had researched. The equivalent thermal conductance of the building blocks shows, that the filled blocks always have lower values. Only the 44T geometry block recommended to use with perlite filler, and PUR foam and aerogel can significantly lower the values of all building blocks. Standardized steady-state condition simulations of temperature and relative humidity distribution in the 44T geometry along line shows that there can be around 6 °C temperature and almost 30 % relative humidity difference inside the blocks regarding the fillers, and better insulating fillers can significantly increase the frost risk zone of the masonry blocks. It is also observable that the temperature along line is almost straight when the hollows are empty, but getting more and more closer to exponential form when the hollows are filled with insulating materials. Better insulating fillers reduce the average temperature of the filled masonry blocks. Use of hydrophobic filler materials at least till 90 % relative humidity is essential in the Nordic countries and till 80% elsewhere. In European climate conditions, filled masonry blocks can perform well against building energetic requirements.

References

- [1] Kreh, R.T., *Masonry Skills*, Cengage Learning, USA (2015)
- [2] Nagy, B., Orosz, M., Optimized thermal performance design of filled ceramic masonry blocks, *Applied Mechanics and Materials* vol. 797 (2015), 174-181
- [3] <http://www.cabotcorp.com/>
- [4] Nagy, B., Tóth, E., Horváth, L., Effect of the fire protection claddings on the temperature change of the structures of industrial buildings, *Acélszerkezetek – Journal of the Hungarian Steel Structure Association* vol. 2015/1 (2015), 6-12
- [5] Krus, M., *Moisture Transport and Storage Coefficients of Porous Mineral Building Materials*, Dissertation, Universität Stuttgart (1995)
- [6] van Schijndel, A.W.M., The Effect of Micro Air Movement on the Heat and Moisture Characteristics of Building Constructions, *Journal of Civil Engineering and Architecture* vol. 4. (2010) 9-15
- [7] van Schijndel, A.W.M., HAM Construction modelling using COMSOL with MatLab, *Proceeding of the COMSOL Users Conference 2006*, Eindhoven (2006)
- [8] Hagentoft, C.-E., Assessment Method of Numerical Prediction Models for Combined Heat, Air and Moisture Transfer in Building Components: Benchmarks for One-dimensional Cases, *Journal of Building Physics* vol. 27. (2004) 327-352
- [9] Künzeli, H.M., *Simultaneous Heat and Moisture Transport in Building Components*, Dissertation, Universität Stuttgart (1994)
- [10] Li, Q., Rao, J., Fazio, P., Development of HAM tool for building envelope analysis, *Building and Environment* vol. 44. (2009) 1065-1073
- [11] Autodesk AutoCAD® 2015, Autodesk Inc. (2015)
- [12] Comsol Multiphysics® 5.0, Comsol Inc. (2015)
- [13] <http://www.amsz.hu>
- [14] <http://remotelab.energia.bme.hu/>
- [15] WUFI® PRO, Fraunhofer IBP (2015)